Journal of Mechanical Engineering Research and Developments
ISSN: 1024-1752
CODEN: JERDFO
Vol. 43, No. 2, pp. 413-421
Published Year 2020

Finite Element Analysis of Heat Flow and Temperature Distribution Inside Cutting Tool

Suhair G. Hussein & Mohammad Qasim Abdullah

Mechanical Engineering Department, University of Baghdad, Iraq

*E-mail: suhair.g.hussein@coeng.uobaghdad.edu.iq

ABSTRACT: Turning stands for a significant machining procedure in which a single-point cutting tool eliminates material from the surface of a rotating cylindrical work piece and the studying of cutting temperature is important because the high temperature lead to reduce tool life. The goal of the current research article is to create a FEM simulation model in order to obtain numerical solutions for temperature distribution occurred at different regions through cemented carbide cutting tool insert. Temperature at tool-chip interface is determined by using empirical relation, it considered as boundary conditions in one side of insert. Finite element method was used as a numerical solution to calculate the temperature distribution at was given boundary conditions that specified. CUMSOLT simulation show the contour of temperature distribution in cutting tool insert.

KEYWORDS: Cemented carbide tools; Temperature distribution; Finite element method (FEM).

INTRODUCTION

Machining process has great rule in manufacturing, turning is regarded as an important one. In this process, the cutting tool has feeding linearly in the parallel direction to the rotation axis [1]. Lathe machine was used in turning process. Three imperative parameters in the process are cutting speed, feeding rate, and cutting depth [2]. Orthogonal and oblique are two expected models in machining process, in which the oblique are is the most machining process while the orthogonal are easier for simulating and it be useful to understand the basic mechanics of machining processes [3].

(A) Cutting temperature

The energy generated during machining process converted to heat by 98% while 2% is related to elastic energy in chip. The temperature of cutting tool end reaches higher than 600°C (873K), this elevated temperature leads to decrease the life of tool and achieving inaccuracies in the dimensions of the machined parts [4] .

(B) Heat generation in machining

High temperature cutting tool affect badly its wear resistance so reducing its life. So, it is important to study a modification for the properties of tool material such as hardness[5]. Investigation of wear and failure features of a tool as a result of temperature developing through cutting process are necessary to quantify. In machining operations, mechanical work has been transformed to heat by the involved plastic deforming in chip creation and by friction amid the tool and work piece. Figure 1 depicts 3 zones of heat generated due to turning, which are named as shear, chip-tool interface as well as the tool-work piece interface regions [6]:

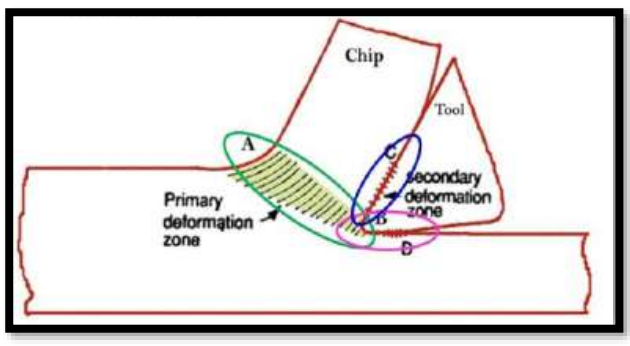

Figure 1. Heat generation and dissipation zones throughout the process of metal cutting [6].

1. The shear zone (primary deformation zone): The shear zone stands for the foremost plastic deforming attributable to shear energy. This heat increases the chip temperature. Some of this heat has been carried away as a result of the chip as it transfers upward along the tool. For a continuous type chip, as the cutting speed raises for a specified feed rate, the chip thickness lessens and less shear energy has been essential for chip deforming so that the chip has heated less from this deforming. About 80-85% of the generated heat in shear zone.

2. The chip-tool interface zone (Secondary deformation zone): It represents a deformation by reason of friction amid the heated chip and tool takes place. This generates an additional rise in the chip temperature. This chip-tool interface gives about 15-20% of heat generated

3. The tool-work piece interface zone: It represents zone D, at flanks in whch frictional rubbing occurs. This area has about 1 to 3% of generated heat. As this heat portion flows into the tool , it produces excessive temperature in area of tool tip which sequentially lessens the tool material hardness. In extreme case , may even produce melting. The wear rate of tool for that reason raises, resultant in a reduction in the advantageous life the tool. It is steadily imperative to comprehend how Machining temperature is influenced by the involved process variable in terms of cutting speed, feed rate, and tool geometry.

G. F. Alabi, T. K. Ajiboye and H.D. Olusegun conducted the study on finite element modelling which has been employed for simulating the temperature distributing for orthogonal cutting of medium carbon steel exposed to numerous methods of heat treatment processes. For all samples that they have been conducted, excessive and restricted temperatures have detected at the tool-chip interface because of a thorough friction model and the shearing action within the cutting zone [8]. Uzorh Augustine .C and ,NwufoOlisaemeka .C addressed a concept to determine the problem of temperature and heat flux at tool-chip interface they used a technique called Inverse heat conduction, proved that at any cutting interface heat flux estimation can calculate temperature field from any region of tool set. They also proposed algorithms that can also be used in selecting various parameters in order to reduce excess thermal load on tool [9]. Majumdar et al, studied the impacts of the heat generation throughout machining operation processes and their consequences on cutting forces and tool wear. In order to study this they have built a fem based computational model to regulate the temperature spreading in a metal cutting process on high-speed carbon steel. Outcomes have shown that as cutting speed rises from 29.6 to 155.4 m/min, the highest temperature in the tool will be correspondingly increased from 709.36 to 1320 K [10].

This paper aims to produce a FEM simulation model for obtaining numerical solutions for temperature distribution at diverse regions through cemented carbide cutting tool insert. Temperature at tool-chip interface has clarified by using empirical relation, it considered as boundary conditions in one side of insert. Finite element method has adopted as a numerical solution to calculate the temperature distribution at specified boundary conditions.

EMPIRICAL RELATION OF ESTIMATION THE CUTTING TEMPERATURE

There are several empirical methods to estimate cutting temperature . One of these method is Cook method that has been derived by means of investigational data for an assortment of work materials to determine parameter values for resultant equation. The equation is feasibly employed to envisage the intensification in temperature at the tool-chip interface throughout machining. [4]

$$\Delta T = \frac{0.4\,U}{\rho C}\left(\frac{v t_c}{K}\right)^{0.333} \qquad (1)$$

Where ΔT = mean temperature rise at the tool –chip interface , °C ; U = specific operation energy ,N-m/mm^3; v= cutting speed, m/s ; t_c= chip thickness before the cutting ,m ; ρc = volumetric specific heat of the tested material, J/mm^3-C = thermal diffusivity of the tested material , m^2/s.

NUMERICAL THERMAL INVESTIGATION FOR CUTTING TOOL INSERT (CTI)

A numerical investigation based on mathematical modeling of FEM by using COMSOLT had been adopted to analyze the temperature distribution and heat flow inside cutting tool insert. An insert of SNUN 120408 specification of 12×12×04 mm3 volume (see figure 2) has been made with thermal conductivity (k) of 84 WmK-1. At that point, meshing of insert has organized and the area where the contact between work piece and tool will take place to make much denser and achieve superior temperature profile.

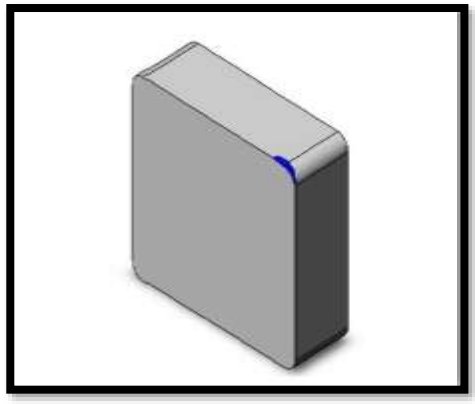

Figure 2. Tool insert

Thermal Governing Equations for CTI: [11]

For developing the governing equations , we express a differential element of a solid body that has a trivial dimension in the z direction , as in figure 3 , and inspect the attitude of conservation of energy for the differential element .As we currently manage dual dimensions, all derivatives have been partial derivatives. Under the supposition of steady state condition (i.e., ΔU = 0), we get:

$$q_x\ t\ dy + q_y\ t\ dx + Q\ t\ dy\ dx = \left(q_x + \frac{\partial q_x}{\partial x}\ dx\right) t\ dy + \left(q_y + \frac{\partial q_y}{\partial y}\ dy\right) t\ dx +$$

$$2h(T - T_a)dydx \qquad (2)$$

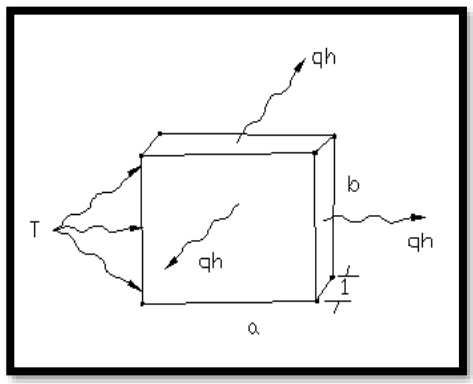

Figure 3. 2D conduction with face and edge convection.

Where

t= thickness

h= the convection coefficient from the surfaces of the differential component

$Ta =$ the ambient temperature of the surrounding fluid

Applying Fourier's principle in the coordinate directions

$$q_x = -k_x\ \frac{\partial T}{\partial X} \qquad (3)$$

$$q_Y = -k_Y\ \frac{\partial T}{\partial Y} \qquad (4)$$

Then substituting and simplifying yields

$$\frac{\partial}{\partial x}\left(tk_x\ \frac{\partial T}{\partial X}\right) + \frac{\partial}{\partial y}\left(tk_Y\ \frac{\partial T}{\partial Y}\right) + Q_t = 2h(T - T_a) \qquad (5)$$

Equation (5) is the leading equation for 2 D conduction with convection from the surface of the tool insert

Finite Element Modeling of CTI

In emerging a finite element method to 2 D conduction with convection, we take a common approach primarily, that is a particular element geometry has not employed. As an alternative, we adopt 2 D element with M nodes such that the temperature distribution in the element can be expressed by

$$T(x,y) = \sum_{i=1}^{\mathrm{M}} Ni(X,y)Ti = (N)(T) \tag{6}$$

where $Ni(X,y)$ is the interpolation function associated with nodal temperature Ti , $[N]$ represents the raw matrix of interpolation function , and $\{T\}$ stands for the column matrix(vector) of nodal temperature .

The element conduction matrix is given by

$$\iint_A \left(K_x \left[\frac{\partial N}{\partial x}\right]^T \left[\frac{\partial N}{\partial x}\right] + K_y \left[\frac{\partial N}{\partial y}\right]^T \left[\frac{\partial N}{\partial y}\right]\right)\{T\}t\, dA + 2h \iint_A [N]^T [N]\{T\}\, dA \tag{7}$$

Which is of the form

$$\left[k^{(e)}\right]\{T\} = \left\{f_h{}^{(e)}\right\} + \left\{f_Q{}^{(e)}\right\} + \left\{f_g{}^{(e)}\right\} \tag{8}$$

As desired.

Comparison of Equations (7) and (8) displays that the conductance matrix is

$$\left[k^{(e)}\right] = \iint_A \left(K_x \left[\frac{\partial N}{\partial x}\right]^T \left[\frac{\partial N}{\partial x}\right] + K_y \left[\frac{\partial N}{\partial y}\right]^T \left[\frac{\partial N}{\partial y}\right]\right) t\, dA + 2h \iint_A [N]^T [N]\, dA \tag{9}$$

The element forcing functions have expressed in column matrix (vector) form as

$$\left\{f_Q{}^{(e)}\right\} = \iint_A Q[N^T]\, t\, dA = \iint_A Q\{N\}\, t\, dA \tag{10}$$

$$\left\{f_h{}^{(e)}\right\} = 2hT_a \iint_A [N]^T\, dA = 2hT_a \iint_A N\, dA \tag{11}$$

$$\left\{f_g{}^{(e)}\right\} = -\oint_S q_s\, n_s\, [N]^T\, t\, ds = -\oint_S q_s\, n_s\, \{N\} t\, ds \tag{12}$$

Where the element conductance matrix is in this case specified by

$$\left[k^{(e)}\right] = \iint_A \left(K_x \left[\frac{\partial N}{\partial x}\right]^T \left[\frac{\partial N}{\partial x}\right] + K_y \left[\frac{\partial N}{\partial y}\right]^T \left[\frac{\partial N}{\partial y}\right]\right) t\, dA + 2h \iint_A [N]^T [N]\, dA$$

$$+h \oint_s [N]^T [N]\, t\, ds \tag{13}$$

Here, the explicitly include edge convection on portion (s)of the element boundary to a subjected convection.

Figure (4) shows four element with element and global node number

As the numbering scheme is chosen , we have constant temperature conditions at global nodes 1, 2 and 3 such that

$T_1 = T_2 = T_3 = 626$ K

Whereas on the other edge , we have convection boundary condition that necessitate a little of investigation to be applied .

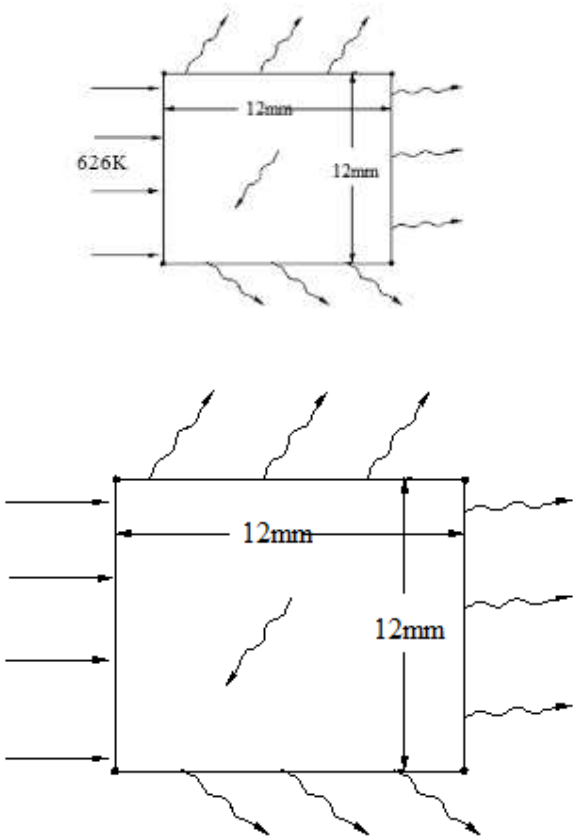

Figure 4_a. Two dimensional insert

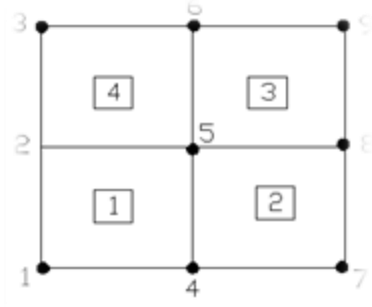

Figure 4_b. Finite element model.

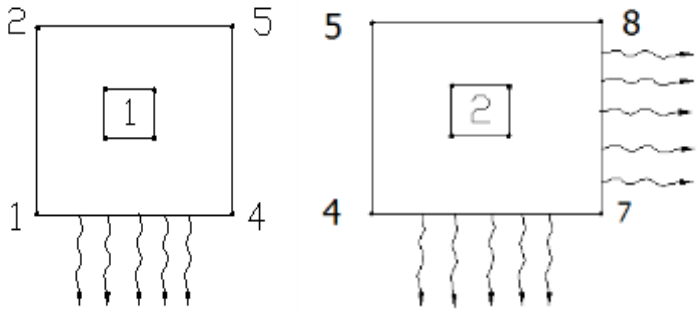

Figure 5. Element nodes

$$N_1(r,s) = \frac{1}{4}(1-r)(1-s) \quad (14)$$

$$N_2(r,s) = \frac{1}{4}(1+r)(1-s) \quad (15)$$

$$N_3(r,s) = \frac{1}{4}(1+r)(1+s) \quad (16)$$

$$N_4(r,s) = \frac{1}{4}(1-r)(1+s) \quad (17)$$

Supposing that k_x and k_y are constant , we have

$$K_{ij} = k_x\, t\frac{b}{a}\int_{-1}^{1}\int_{-1}^{1}\frac{\partial N_i}{\partial r}\frac{\partial N_j}{\partial r}\,dr\,ds + k_y\, t\frac{a}{d}\int_{-1}^{1}\int_{-1}^{1}\frac{\partial N_i}{\partial r}\frac{\partial N_j}{\partial r}\,dr\,ds + 2hab\int_{-1}^{1}\int_{-1}^{1}N_i\,N_j\,dr\,ds \quad i,j = 1,4 \quad (18)$$

The global equation for the four element model can in this case be accumulated by entering the element –to-global nodal correspondence relation as

$$\left[L^{(1)}\right] = [1 \quad 4 \quad 5 \quad 2]$$

$$\left[L^{(2)}\right] = [4 \quad 7 \quad 8 \quad 5]$$

$$\left[L^{(3)}\right] = [5 \quad 8 \quad 9 \quad 6]$$

$$\left[L^{(4)}\right] = [2 \quad 5 \quad 6 \quad 3]$$

The element stiffness matrices as

$$\left[k_e^{(1)}\right] = \begin{bmatrix} .224 & .056 & -.122 & .168 \\ -.056 & .224 & -.168 & -.128 \\ -.112 & -.168 & .224 & .224 \\ -.168 & -.128 & -.056 & .224 \end{bmatrix}$$

$$\left[k_e^{(2)}\right] = \begin{bmatrix} .224 & .056 & -.122 & .168 \\ -.056 & .224 & -.168 & -.128 \\ -.112 & -.168 & .224 & .224 \\ -.168 & -.128 & -.056 & .224 \end{bmatrix}$$

$$\left[k_e^{(3)}\right] = \begin{bmatrix} .224 & .056 & -.122 & .168 \\ -.056 & .224 & -.168 & -.128 \\ -.112 & -.168 & .224 & .224 \\ -.168 & -.128 & -.056 & .224 \end{bmatrix}$$

$$\left[k_e^{(4)}\right] = \begin{bmatrix} .224 & .056 & -.122 & .168 \\ -.056 & .224 & -.168 & -.128 \\ -.112 & -.168 & .224 & .224 \\ -.168 & -.128 & -.056 & .224 \end{bmatrix}$$

Employing the direct assembly-superposition process with the element to global node transfer relations, the global conductance matrix will be:

$$[k_e] = 10^3 \times \begin{bmatrix} .224 & .168 & 0.00 & -.056 & -.112 & 0.00 & 0.00 & 0.00 & 0.00 \\ -.168 & .448 & -.168 & -.128 & -.112 & -.112 & 0.00 & 0.00 & 0.00 \\ 0 & .168 & .224 & 0.00 & -.128 & -.056 & 0.00 & 0.00 & 0.00 \\ -.056 & -.128 & 0.00 & .448 & -.336 & 0.00 & -.056 & -.112 & 0.00 \\ -.112 & -.112 & -.128 & -.336 & .896 & -.336 & -.128 & -.112 & -.112 \\ 0 & -.112 & -.056 & 0.00 & -.168 & .448 & 0.00 & -.128 & -.056 \\ 0 & 0 & 0.00 & -.056 & -.128 & 0.00 & .224 & -.168 & 0.00 \\ 0 & 0 & 0.00 & -.112 & -.112 & -.128 & -.168 & .448 & -.168 \\ 0 & 0 & 0.00 & 0.00 & -.112 & -.056 & 0.00 & -.168 & .224 \end{bmatrix}$$

The nodal temperature vector is

$$\{T\} = \begin{bmatrix} 626 \\ 626 \\ 626 \\ T_4 \\ T_5 \\ T_6 \\ T_7 \\ T_8 \\ T_9 \end{bmatrix}$$

And we have obviously incorporated the prearranged temperature boundary conditions, observing that no internal heat is produced, we get :

$$\{F\} = \begin{bmatrix} 505.6 + F_1 \\ 1011.2 + F_2 \\ 505.6 + F_3 \\ 1011.2 \\ 1338.8 \\ 1011.2 \\ 683 \\ 1011.2 \\ 683 \end{bmatrix}$$

Where $F_1, F_2,$ and F_3 are heat flux constituents at node 1,2,and 3.

RESULTS AND DISCUSSION

By using eq.(1) temperature at the tool chip interface had been obtained as (626 K). This temperature considered as a boundary conditions that used in formulation FEM to calculate temperature distribution inside the cutting tool.

Simultaneous solution of the global equations yields the nodal temperature as

$$\begin{Bmatrix} T_4 \\ T_5 \\ T_6 \\ T_7 \\ T_8 \\ T_9 \end{Bmatrix} = \begin{Bmatrix} 542 \\ 614 \\ 582 \\ 498 \\ 582 \\ 498 \end{Bmatrix} \text{ K}$$

If substitute the computed nodal temperature into the 1st three of the global equations, explicitly, the heat flow as

$$\begin{Bmatrix} F1 \\ F2 \\ F3 \end{Bmatrix} = \begin{Bmatrix} 1351.6 \\ 3954.5 \\ 1351.6 \end{Bmatrix} w/m$$

From COMSOL analysis the temperature distribution for CTI had been obtained as shown in Figure.6. The red color indicates the highest value of temperature distribution, while blue regions indicates the lowest one. Figure 7 depicts Contour temperature in CTI by using COMSOLT simulator.

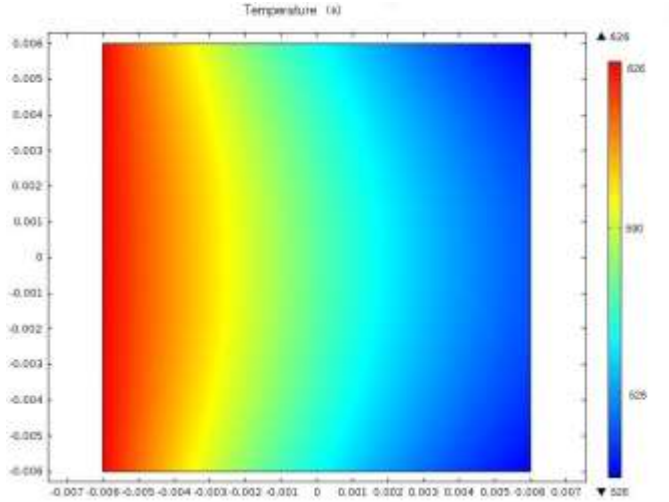

Figure 6. temperature distribution in CTI by using COMSOLT program

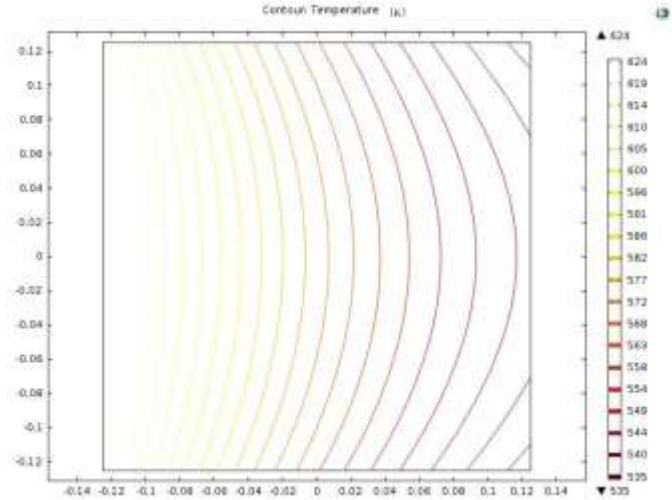

Figure 7. Contour temperature in CTI by using COMSOLT program

CONCLUSION

Finite element method was used as a numerical solution to calculate the temperature distribution inside cutting tool insert and it considered as a suitable solution to predict the temperature distribution inside cutting tool insert by CUMSOLT simulator ranged from red to blue regions indicating the range of maximum to minimum values of temperature distribution. This simulator as well shows the contour of temperature distribution in cutting tool insert.

REFERENCES

[1] S. Dahbi, H. EL Moussami, L. Ezzine. "Optimization of turning parameters for surface roughness", *HAL Id: hal-01260818 https://hal.archives-ouvertes.fr/hal-01260818* Submitted on 22 Jan. 2016

[2] S.S. Chaudhari, S.S. Khedkar, N.B. Borkar. "Optimization of process parameters using Taguchi approach with minimum quantity lubrication for turning". *International Journal of Engineering Research and Applications (IJERA)*. 1, No. 4, PP.1268-1273. 2011

[3] H. Pathak, S. Das, R. Doley, & S. Kashyap. "Optimization of Cutting Parameters for AISI H13 Tool Steel by Taguchi Method and Artificial Neural Network". In *Deep Learning and Neural Networks: Concepts, Methodologies, Tools, and Applications* (pp. 531-551). IGI Global. 2020

[4] M.P. Groover. "Principles of Modern Manufacturing: SI Version". *Wiley*. 2013

[5] G.M. Wani, N.C. Ghuge. "Thermal Analysis Of Single Point Cutting Tool Using Different Cutting Conditions". *International Journal of Informative & Futuristic Research*, vol. 3, no. 9, pp. 3472-3483, May. 2016

[6] Y.R. Bhoyar, P.D. Kamble. "Finite Element Analysis on Temperature Distribution of Turning Process". *International Journal of Modern Engineering Research (IJMER)*, vol. 3, no. 1, pp.541-546. 2013

[7] M. Pradeep Kumar, K. Amarnath, M. Sunil Kumar. "A Review on Heat Generation in Metal Cutting". *International Journal of Engineering and Management Research*, Vol.5, no. pp. 193-197. August. 2015

[8] A.G.F. Alabi, T.K. Ajiboye, H.D. Olusegun. "Investigation of Cutting Temperatures Distribution in Machine Heat Treated Medium Carbon Steel on a Lathe". *The Pacific Journal of Science and Technology*, vol. 13, no. 1, May. 2012

[9] C. Uzorh Augustine, O. Nwufo. "Thermal Aspect of Machining: Evaluation of Tool and Chip Temperature during Machining Process Using Numerical Method" *The International Journal Of Engineering And Science (IJES)*, vol. 2, no. 4, pp. 66-79. 2013

[10] M. Pradip, R. Jayaramachandran, S. Ganesan. "Finite element analysis of temperature rise in metal cutting Processes" *Applied Thermal Engineering*, vol. 25, pp. 2152–2168. 2005

[11] D.V. Hutton. "Fundamentals of finite element analysis". *McGraw-hill*. 2017.